Journal of Inorganic Biochemistry 105 (2011) 435–443

Contents lists available at ScienceDirect

Journal of Inorganic Biochemistry

journal homepage: www.elsevier.com/locate/jinorgbio

The interesting DNA-binding properties of three novel dinuclear Ru(II) complexes with varied lengths of flexible bridges

Chuan-Chuan Ju, An-Guo Zhang, Chui-Li Yuan, Xiao-Long Zhao, Ke-Zhi Wang *

College of Chemistry, Beijing Normal University, Beijing 100875, China

ARTICLE INFO

Article history:
Received 10 January 2010
Received in revised form 11 December 2010
Accepted 14 December 2010
Available online 29 December 2010

Keywords:
Ruthenium
Bipyridine
Phenanthroline
DNA

ABSTRACT

Three binuclear Ru(II) complexes with two $[Ru(bpy)_2(pip)]^{2+}$-based subunits {where bpy = 2,2′-bipyridine and pip = 2-phenylimidazo[4,5-*f*][1,10]phenanthroline} being linked by varied lengths of flexible bridges, were synthesized and characterized by ^{1}H NMR, elemental analysis, UV–visible (UV–vis) and photoluminescence spectroscopy. The structures of the three complexes were optimized by density functional theory calculations. The interaction of the complexes with calf thymus DNA was investigated by UV–vis and luminescence titrations, steady-state emission quenching by $[Fe(CN)_6]^{4-}$, DNA competitive binding with ethidium bromide, DNA melting experiments, and viscosity measurements. The experimental results indicated that the three complexes bound to the DNA most probably in a threading intercalation binding mode with high DNA binding constant values three orders of magnitude greater than the DNA binding constant value reported for proven DNA intercalator, mononuclear counterpart $[Ru(bpy)_2(p\text{-mopip})]^{2+}$ {*p*-mopip = 2-(4-methoxylphenyl)imidazo[4,5-*f*][1,10] phenanthroline}.

1. Introduction

Ruthenium(II) polypyridyl complexes have been investigated substantially because of their extensive applications in the field of photochemistry, photophysics, and bioinorganic chemistry in the past decades [1,2]. Due to their excellent chemical stability, facile electron transfer, strong luminescent emission, and relatively long-lived excited states, Ru(II) complexes have attracted much attention as the DNA structural probes, DNA footprinting, and sequence specific cleaving agents [3–6]. However, most of these Ru(II) complexes are mononuclear [7–16]. There are some significant drawbacks for mononuclear Ru(II) complexes as DNA binders and structural probes. For example, if metal complexes are to approach the binding footprint of a DNA-binding protein, the recognition of at least 8–10 base pairs is essential. The complexes need to possess high DNA-binding affinity at high ionic strength condition (such as 150 mM NaCl) [17,18]. However, the mononuclear Ru(II) complexes are relatively small and can only span 1–2 DNA base pairs. Commonly, these mononuclear complexes have weak DNA-binding affinity ($K_b \approx 10^4 - 10^6\ M^{-1}$, depending on the intercalators) and are easily displaced from DNA at high ionic strength [19,20]. Dinuclear Ru(II) complexes could overcome above-mentioned drawbacks as they have increased size, charge, varied molecular shapes, and greater DNA-binding affinity. However, a limited number of dinuclear Ru(II) complexes have been reported for the DNA-binding studies [17,18,21–41].

Dinuclear Ru(II) complexes carrying a bridging ligand can be classified into rigid and flexible ones according to the linking bridge type. The binding to double-strand DNA by the two metal centers of dinuclear complexes with rigid bridges are usually limited by their rigidity. Because the two metal centers are rigidly linked and consequently can not follow the curvature of the DNA, only one metal center may bind deeply to the DNA with the second metal center projecting out of the DNA [21–34]. The other kind of dinuclear Ru(II) complexes carrying a flexible chain should overcome the limitations and potentially allow both the metal centers to bind optimally to the DNA [35–41]. Since the chain length of the linker for dinuclear Ru(II) complexes has been reported to be a crucial factor in determining the binding efficiency [17], we have synthesized three novel dinuclear Ru (II) complexes with different lengths of flexible bridges as linkers of the two $[Ru(bpy)_2(pip)]^{2+}$ {bpy = 2,2′-bipyridine; pip = 2-phenylimidazo [4,5-*f*][1,10]phenanthroline}-based subunit [42], and studied their DNA binding properties.

2. Experimental

2.1. Materials

cis-$[Ru(bpy)_2Cl_2]\cdot 2H_2O$ [43] and 1,10-phenanthroline-5,6-dione [44] were prepared according to the literature routes. The three dinuclear Ru(II) complexes **1–3** used in this study, were synthesized according to a modified literature method for the synthesis of an

* Corresponding author. Tel.: +86 10 58805476; fax: +86 10 58802075.
E-mail address: kzwang@bnu.edu.cn (K.-Z. Wang).

0162-0134/$ – see front matter © 2010 Elsevier Inc. All rights reserved.
doi:10.1016/j.jinorgbio.2010.12.004

analogous Ru(II) complex [45]. The synthetic route is shown in Scheme 1, and the synthetic details are described below. Other materials were commercially available and used without further purification.

2.2. Physical measurements

^{1}H NMR spectra were collected with a Bruker DRX-400 NMR spectrometer with $(CD_3)_2SO$ as the solvent at room temperature. All chemical shifts were given relative to tetramethylsilane. The following symbols are used in NMR spectral description: s (singlet), d (doublet), dd (doublet of doublets), dt (doublet of triplets), and t (triplet). The microanalyses (C, N, and H) were performed with a Vario EL elemental analyzer.

All solutions involving DNA experiments, were prepared by thrice distilled water. A solution of calf thymus DNA (ct-DNA) gave ratios of UV absorbance at 260 and 280 nm of about 1.9:1, indicating that the DNA is sufficiently free of protein [46]. The DNA concentrations per nucleotide were determined spectrophotometrically by assuming

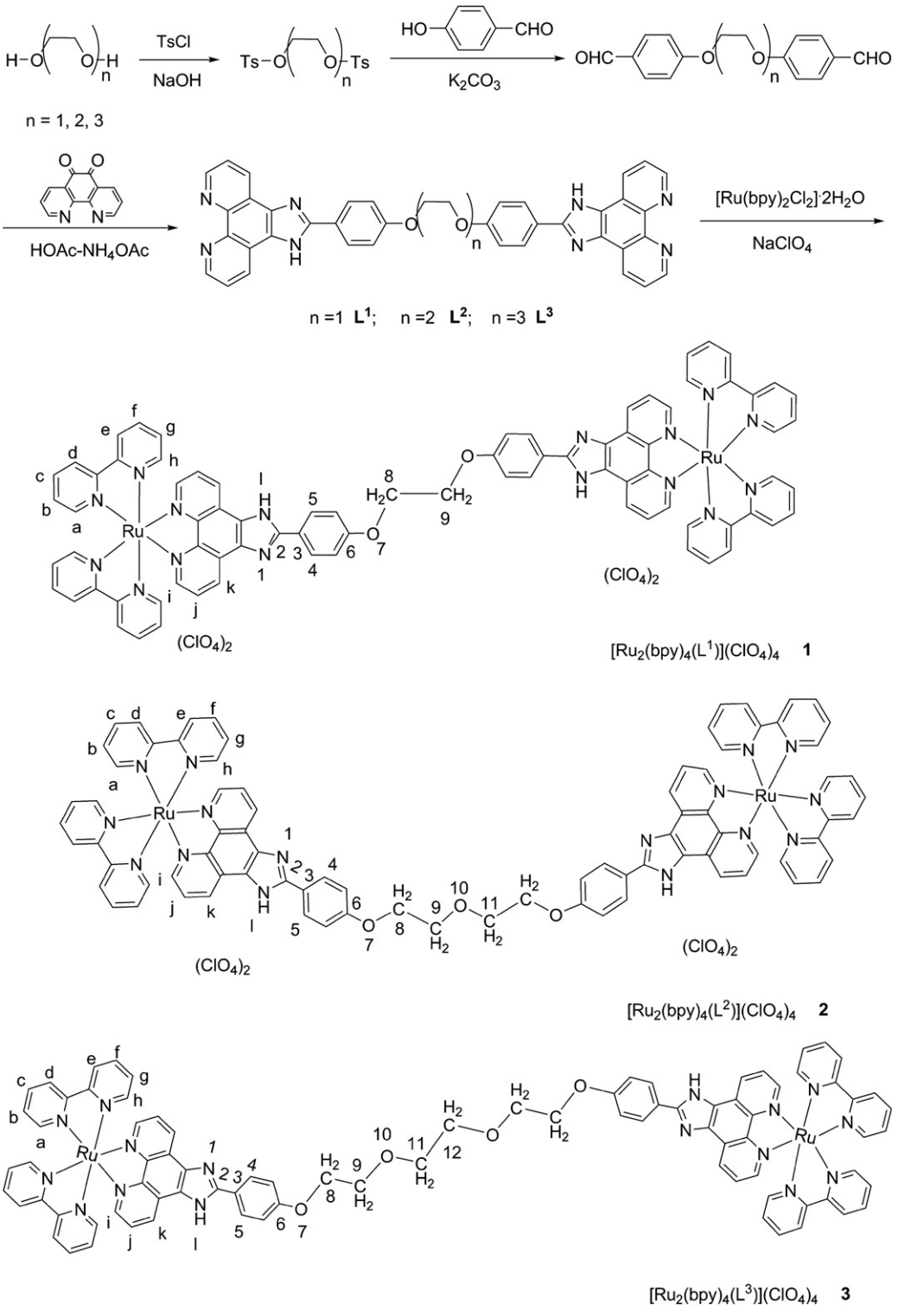

Scheme 1. Synthetic route to **1**–**3** and proton numbering scheme.

$\varepsilon_{260\,nm} = 6600\ M^{-1}\,cm^{-1}$ [47]. UV–visible (UV–vis) absorption spectra were recorded on a GBC Cintra 10e UV–vis spectrophotometer. Emission spectra were obtained on a Varian Cary Eclipse fluorescence spectrometer. The titrations were carried out by using 1-cm-path quartz cuvettes at room temperature of 20 °C unless otherwise mentioned, in Tris–HCl buffer (5 mM Tris–HCl, 50 mM NaCl, pH = 7.10) by keeping the concentrations of the complexes constant while varying the DNA concentrations. After the solutions of the Ru(II) complexes were allowed to incubate with the DNA for 10 min, the UV–vis spectra were measured by using the buffer containing same amounts of the DNA as the reference blanks. The values of intrinsic binding constant K_b illustrating the binding strength of the complex with ct-DNA, and the binding site size s were determined by fitting the titration data to Eqs. (1) and (2) [48,49]

$$\frac{\varepsilon_a-\varepsilon_f}{\varepsilon_b-\varepsilon_f} = \frac{b-\sqrt{b^2-\frac{2K_b^2C_t[DNA]}{s}}}{2K_bC_t} \quad (1)$$

$$b = 1 + K_bC_t + \frac{K_b[DNA]}{2s} \quad (2)$$

where [DNA] is the concentration of DNA in base pairs, ε_a, ε_f, and ε_b are the apparent, free, and bound metal complex extinction coefficients, respectively, s is the binding site size in base pairs, and C_t is the total Ru (II) complex concentration.

Steady-state emission quenching experiments were carried out in the Tris–HCl buffer by using $K_4[Fe(CN)_6]$ as the quencher. The experiments of DNA competitive binding with ethidium bromide (EB) were carried out also in Tris–HCl buffer by keeping [DNA]/[EB] = 5 and varying the concentrations of the Ru(II) complexes.

Thermal denaturation experiments were performed on a UV–vis spectrophotometer in a phosphate buffer (1.5 mM Na_2HPO_4, 0.5 mM NaH_2PO_4, 0.25 mM Na_2EDTA, pH = 7.0). With the use of the thermal melting program, the temperature of the cell containing the cuvette was ramped from 50 to 90 °C at a rate of 1 °C min^{-1}, and the absorbance at 260 nm was measured every 0.5 °C.

The viscosity measurements were carried out using an Ubbelodhe viscometer immersed in a thermostated water bath maintained at 32.04 ± 0.02 °C. The DNA samples for viscosity measurements were prepared by sonication in order to minimize complexities arising from DNA flexibility [50]. The flow time was measured, and each sample was measured at least five times, and an average flow time was calculated. Data were presented as $(\eta/\eta_0)^{1/3}$ vs [Ru]/[DNA], where η is the viscosity of DNA in the presence of the Ru(II) complex and η_0 is the viscosity of the DNA solution alone.

2.3. Synthesis

2.3.1. Ethane-1,2-diyl bis(4-methylbenzenesulfonate)

A mixture of ethane-1,2-diol (1.25 g, 20 mmol), 4-methylbenzene-1-sulfonyl chloride (TsCl) (9.5 g, 50 mmol) and sodium hydroxide (2.0 g, 50 mmol) was ground for about 10 min in mortar. Then a white powder gained, was washed with water several times and then dried in vacuo. The product was directly used for following synthesis without further purification.

2.3.2. 2,2′-Oxybis(ethane-2,1-diyl) bis(4-methylbenzenesulfonate)

This was synthesized as described above for ethane-1,2-diyl bis(4-methylbenzenesulfonate) except that 2,2′-oxydiethanol was used instead of ethane-1,2-diol.

2.3.3. 2,2′-(Ethane-1,2-diylbis(oxy))bis(ethane-2,1-diyl) bis(4-methylbenzenesulfonate)

This was synthesized as described above for ethane-1,2-diyl bis(4-methylbenzenesulfonate) except that 2,2′-(ethane-1,2-diylbis(oxy)) diethanol was used instead of ethane-1,2-diol.

2.3.4. 4,4′-[1,2-Ethanediylbis(oxy)]bis-benzaldehyde

To a mixture of 4-hydroxybenzaldehyde (2.07 g, 17 mmol) and potassium carbonate (2.35 g, 17 mmol) in 100 ml *N,N*-dimethylformide, was dropwise added ethane-1,2-diylbis(4-methylbenzenesulfonate) (2.74 g, 8 mmol) in *N,N*-dimethylformide (150 ml) during a period of 20 min at constant stirring under the protection of N_2 at room temperature. The reaction mixture was heated at 80 °C under stirring for 24 h under the protection of N_2 and then was cooled to room temperature. A brown-yellow powder obtained after the removal of the solvent under a reduced pressure, was directly used for following synthesis without further purification.

2.3.5. 4,4′-(2,2′-Oxybis(ethane-2,1-diyl)bis(oxy))dibenzaldehyde

This was synthesized as described above for 4,4′-[1,2-ethanediylbis(oxy)]bis-benzaldehyde except that 2,2′-oxybis(ethane-2,1-diyl) bis(4-methylbenzenesulfonate) was used instead of ethane-1,2-diylbis(4-methylbenzenesulfonate).

2.3.6. 4,4′-(2,2′-(Ethane-1,2-diylbis(oxy))bis(ethane-2,1-diyl))bis(oxy) dibenzaldehyde

This was synthesized as described above for 4,4′-[1,2-ethanediylbis(oxy)]bis-benzaldehyde except that 2,2′-(ethane-1,2-diylbis(oxy))bis(ethane-2,1-diyl)bis(4-methylbenzenesulfonate) was used instead of ethane-1,2-diylbis(4-methylbenzenesulfonate).

2.3.7. 1,2-Bis(4-(1H-imidazo[4,5-f][1,10]phenanthrolin-2-yl)phenoxy) ethane (L^1)

A mixture of 1,10-phenanthroline-5,6-dione (0.64 g, 3 mmol), 4,4′-[1,2-ethanediylbis(oxy)]bis-benzaldehyde (0.41 g, 1.5 mmol), ammonium acetate (2.3 g, 30 mmol), and glacial acetic acid (25 ml) was refluxed for 6 h. The cooled solution was neutralized to pH = 7.0 with concentrated aqueous ammonia. The precipitate formed was collected by filtration and was recrystallized from DMF-diethyl ether. The resulting solid was directly used for following synthesis without further purification due to solubility problem.

2.3.8. 2,2′-(4,4′-(2,2′-Oxybis(ethane-2,1-diyl)bis(oxy)) bis(4,1-phenylene))bis(1H-imidazo[4,5-f][1,10]phenanthroline) (L^2)

This was synthesized as described above for L^1 except that 4,4′-(2,2′-oxybis(ethane-2,1-diyl)bis(oxy))dibenzaldehyde was used instead of 4,4′-[1,2-ethanediylbis(oxy)]bis-benzaldehyde.

2.3.9. 1,2-Bis(2-(4-(1H-imidazo[4,5-f][1,10]phenanthrolin-2-yl) phenoxy)ethoxy) ethane (L^3)

This was synthesized as described above for L^1 except that 4,4′-(2,2′-(ethane-1,2-diylbis(oxy))bis(ethane-2,1-diyl))bis(oxy)dibenzaldehyde was used instead of 4,4′-[1,2-ethanediylbis(oxy)]bis-benzaldehyde.

2.3.10. $[Ru_2(bpy)_4(L^{1-3})](ClO_4)_4$

A suspension of $[Ru(bpy)_2Cl_2]\cdot 2H_2O$ (0.291 g, 0.6 mmol) and L^{1-3} (0.3 mmol) in ethanol (100 ml) was refluxed under the protection of N_2 for 6 h. After most of the solvent was removed under a reduced pressure, a red precipitate was obtained by the dropwise addition of a 4-fold excess of saturated aqueous $NaClO_4$ solution. The purification was carried out by column chromatography on silica gel with CH_3CN-H_2O-saturated aqueous KNO_3 (40:4:1, v/v/v) as eluent followed by reprecipitation with a saturated $NaClO_4$ aqueous solution. Light-red crystals were obtained in >60% yields. (Caution! All the perchlorate salts are potentially explosive and therefore should be handled in small quantity with care.)

$[Ru_2(bpy)_4(L^1)](ClO_4)_4\cdot 3H_2O$ **1**·$3H_2O$: Yield: 60%. UV–vis in CH_3CN: λ/nm ($\varepsilon/10^5\ M^{-1}\,cm^{-1}$): 287 (2.02); 320 (0.81); 460 (0.37). ^1H NMR (500 MHz, Me_2SO-d_6) (see Scheme 1 for proton numbering scheme): δ 14.22 (s, $2H_l$), 9.10 (d, $4H_k$), 8.87 (dd, $8H_{d,e}$), 8.30 (d, $4H_{4,c}$), 8.23 (t, $4H_{f,i}$), 8.12 (t, $4H_b$), 8.07 (d, $4H_h$), 7.95 (d, $4H_a$),

7.86 (d, $4H_b$), 7.60 (d, $8H_g$), 7.34 (d, $8H_5$), 4.54 (s, $4H_8$). Anal. Calcd for $C_{80}H_{58}Cl_4N_{16}O_{18}Ru_2\cdot 3H_2O$: C, 49.79; H, 3.32; N, 11.62. Found: C, 49.81; H, 3.45; N, 11.49.

$[Ru_2(bpy)_4(L^2)](ClO_4)_4\cdot 4H_2O$ **2**·$4H_2O$: Yield: 65%. UV–vis in CH_3CN: λ/nm (ε/10^5 M^{-1} cm^{-1}): 287 (2.21); 320 (0.73); 460 (0.38). ^1H NMR (500 MHz, Me_2SO-d_6) (see Scheme 1 for proton numbering scheme): δ 14.23 (s, $2H_l$), 9.08 (d, $4H_k$), 8.88 (dd, $8H_{d,e}$), 8.28 (d, $4H_{4,c}$), 8.23 (t, $4H_{f,i}$), 8.12 (t, $4H_b$), 8.06 (d, $4H_h$), 7.94 (d, $4H_a$), 7.85 (d, $4H_a$), 7.60 (t, $8H_b$), 7.35 (t, $4H_g$), 7.28 (d, $4H_5$), 4.30 (s, $4H_8$), 3.94 (s, $4H_9$). Anal. Calcd for $C_{82}H_{62}Cl_4N_{16}O_{19}Ru_2\cdot 4H_2O$: C, 49.45; H, 3.52; N, 11.26. Found: C, 49.66; H, 3.54; N, 11.01.

$[Ru_2(bpy)_4(L^3)](ClO_4)_4\cdot 5H_2O$ **3**·$5H_2O$: Yield: 65%. UV–vis in CH_3CN: λ/nm (ε/10^5 M^{-1} cm^{-1}): 287 (1.99); 320 (0.61); 460 (0.33). ^1H NMR (500 MHz, Me_2SO-d_6) (see Scheme 1 for proton numbering scheme): δ 14.19 (s, $2H_l$), 9.08 (d, $4H_k$), 8.86 (dd, $8H_{d,e}$), 8.25 (t, $8H_{4,c}$), 8.22 (t, $4H_{f,i}$), 8.11 (d, $4H_b$), 8.06 (dt, $4H_h$), 7.85 (d, $4H_a$), 7.60 (t, $8H_b$), 7.34 (t, $4H_g$), 7.27 (d, $4H_5$), 4.26 (s, $4H_8$), 3.85 (s, $4H_9$), 3.70 (s, $4H_{11}$). Anal. Calcd for $C_{84}H_{66}Cl_4N_{16}O_{20}Ru_2\cdot 5H_2O$: C, 49.12; H, 3.70; N, 10.92. Found: C, 49.00; H, 3.84; N, 10.71.

2.4. Computational methods

Each of **1–3** is made of a Ru(II) ion, one of main ligands L^{1-3} and two ancillary ligands bpy. The starting structures of **1–3** were constructed based on the optimized structure of $[Ru(bpy)_2(pip)]^{2+}$ [51]. Geometry optimization computations were performed applying the DFT-B3LYP method [52] and LanL2DZ basis set (ECP + DZ for the Ru atom and D95 for C, N, O, H atoms) [53], and assuming the singlet state for the ground state of the complex [54]. All the computations were performed with the G03 quantum chemistry program-package [55].

3. Results and discussion

3.1. UV–vis absorption spectra

The absorption spectra of **1–3** in the absence and the presence of ct-DNA are shown in Figs. 1, S1, and S2. In the absence of the DNA, UV–vis absorption spectra of the three complexes in water are quite similar to each other, characterized by a bpy-centered π–π* transition band at ~287 nm, and a metal-to-ligand charge transfer (MLCT) transition band at ~465 nm. These assignments are made on the basis of the comparisons of the spectra of **1–3** with that for $[Ru(bpy)_3]^{2+}$ [56]. With increasing concentrations of ct-DNA, **1–3** exhibited smaller hypochromicities of <8% for the MLCT bands than a hypochromicities of 11% reported for corresponding band of an analogous Ru(II) complex of $[Ru(bpy)_2(p\text{-mopip})]^{2+}$ {*p*-mopip = 2-(4-methoxylphenyl)imidazo[4,5-*f*][1,10]phenanthrolin} [15], but more evident hypochromicities of 47%, 39%, and 45% respectively for the π–π* transition bands at 285 nm than a hypochromicity of 34% reported for $[Ru(bpy)_2(p\text{-mopip})]^{2+}$ [15]. The little changes of the MLCT bands observed may be because the MLCT band is mainly Ru-to-bpy charge transfer in nature. Similar behavior was also observed in other dinuclear Ru(II) complexes [22,28,34]. The notable hypochromicities observed for the π–π* transition bands of **1–3** at ~287 nm are much larger than those reported for typical DNA intercalators [57,58] (see Table 1). Hiort et al. ever deduced that the dppz in $[Ru(phen)_2(dppz)]^{2+}$ {phen = 1,10-phenanthroline; dppz = dipyrido[3,2-a:2′,3′-c]phenazine} intercalates between the DNA base pairs because the hypochromism of the intraligand transition of dppz is greater than that of the MLCT [58]. The evident spectral changes observed may suggest that **1–3** exhibit high DNA binding affinity. After binding to the DNA, the π* orbital of the binding ligand could couple with π orbit of base pairs in the DNA. The coupling π* orbital was partially filled by electrons, thus decreasing the transition probabilities, and concomitantly resulting in the hypochromicity [59]. However, the ligand bpy was previously demonstrated to be at best only minimally efficient at inducing intercalative binding with the DNA [60]. The ligand pip-containing mononuclear Ru(II) complex did not exhibit the notable hypochromicity as it intercalated into the DNA [42]. These facts indicate that the flexible bridges between the two Ru^{2+} cores in **1–3** play an important role in the DNA binding. In order to further illustrate the binding strength of the complexes, the values of intrinsic binding constant K_b and the binding site size s with ct-DNA were obtained by monitoring the changes in absorbance at ~287 nm of the Ru(II) complexes, with increasing concentrations of DNA. The K_b and s values of **1–3** were derived to be $K_b = (5.7 \pm 1.6)\times 10^7$ M^{-1} and $s = 1.85 \pm 0.02$ for **1**, $K_b = (7.5 \pm 3.1)\times 10^7$ M^{-1} and $s = 1.47 \pm 0.02$ for **2**, and $K_b = (9.5 \pm 2.5)\times 10^7$ M^{-1} and $s = 0.92 \pm 0.01$ for **3,** from data in the insets of Figs. 1, S1, and S2. The values of hypochromicity and intrinsic DNA binding constant of **1–3** in this study and analogous mononuclear and dinuclear Ru(II) complexes are compared in Table 1. Obviously, the values of the DNA binding constant derived for **1–3** are close to each other within the experimental errors, while s values decease with increasing linker lengths. The similar DNA binding affinities indicate that **1–3** would have similar binding mode, and the strong dependence of s values on the linker lengths of **1–3** suggests that **1–3** interact with the DNA in a threading bis-intercalating binding mode, namely both ends of the complex to bind to the same strand of DNA rather than the interaction with two strands of the DNA through interstrand binding. Kelley [17] reported DNA binding constant

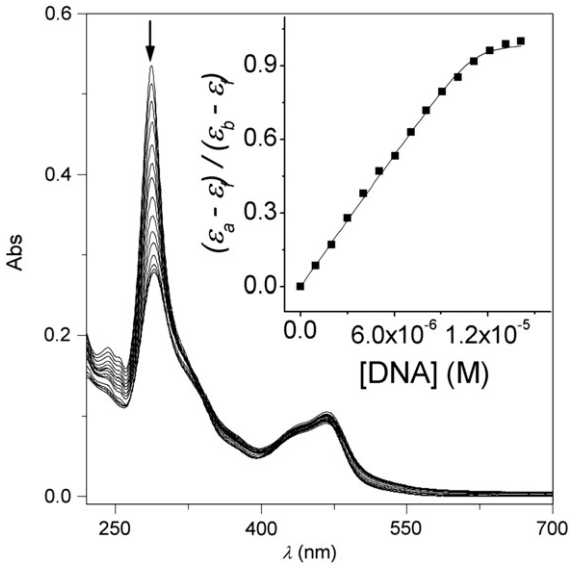

Fig. 1. Changes in UV–vis spectra of 1 (3 μM) with increasing concentrations of ct-DNA in 5 mM Tris–HCl buffer (pH = 7.10, 50 mM NaCl). Arrows show spectral changes upon increasing DNA concentrations.

Table 1
Comparisons of DNA binding parameters.

Complex	H (%) (λ_{max}) (nm)[a]	K_b (M^{-1})	Ref.
$[Ru(bpy)_2(pip)]^{2+}$	22 (458)	4.7×10^5	[42]
$[Ru(bpy)_2(p\text{-hpip})]^{2+}$	34 (264);16 (458)	6.9×10^4	[15]
$[Ru(bpy)_2(p\text{-mopip})]^{2+}$	34% (264);11 (456)	2×10^4	[15]
$[Ru(bpy)_2(dppz)]^{2+}$	14.5 (460)	5.0×10^6	[64]
$[Ru_2(ebipcH_2)(bpy)_4]^{4+}$	36.6 (288)	1.3×10^6	[28]
$[Ru_2(bmbh)(phen)_4]^{4+}$	16 (460)	0.36×10^7	[17]
$[Ru_2(cpdppz)(phen)_4]^{4+}$	–	~10^9	[35]
$[Ru_2(phen\text{-}5\text{-}SOS\text{-}5\text{-}phen)(dpq)_4]^{4+}$	–	$(8.9\pm 4.3)\times 10^7$	[18]
1	45 (287);5 (465)	$(5.7\pm 1.6)\times 10^7$	this work
2	38 (285);5 (465)	$(7.5\pm 3.1)\times 10^7$	this work
3	47 (286);5 (465)	$(9.5\pm 2.5)\times 10^7$	this work

[a] See Abbreviations section. [b] $H\% = 100\times(A_{free} - A_{bound})/A_{free}$.

values of 2.4×10^6, 3.6×10^6 and 3.0×10^6 M^{-1} for dinuclear Ru(II) complexes of $[(phen)_2Ru^{II}(Mebpy)\text{-}(CH_2)_n\text{-}(bpyMe)Ru^{II}(phen)_2]^{4+}$ {Mebpy = 4-methyl-2,2′-bipyridyl-4′-} with n = 5, 7, and 10, respectively. In view of experimental uncertainties, Kelly's DNA binding constant values seem insensitive to the linker lengths. Instead variations in the linker lengths were reported to profoundly affect values of binding site size s, s = 6.4, 8.8, and 6.0 base pairs for the complexes with linker lengths of n = 5, 7, and 10, respectively, which is in agreement with our observation. As shown in Table 1, the K_b values obtained for **1**–**3** are much larger than the K_b values of 4.7×10^5, 1×10^5 and 2×10^4 M^{-1} reported for analogous mononuclear complexes of $[Ru(bpy)_2(pip)]^{2+}$ [42], $[Ru(bpy)_2(p\text{-}hpip)]^{2+}$ {p-hpip = 2-(p-hydroxyphenyl)imidazo[4,5-*f*][1,10]phenanthroline} [61], and $[Ru(bpy)_2(p\text{-}mopip)]^{2+}$ [15], respectively, even larger than the K_b values of 5.0×10^6 and 1.3×10^6 M^{-1} previously reported for a typical DNA intercalator $[Ru(bpy)_2(dppz)]^{2+}$ [62], and a rigid bridge-containing dinuclear complex $[Ru_2(ebipcH_2)(bpy)_4]^{4+}$ {ebipcH$_2$ = N-ethyl-4,7-bis([1,10]-phenanthroline[5,6-*f*]imidazol-2-yl)carbazole}[28], respectively. It is noteworthy that the K_b values for **1**–**3** are one order of magnitude greater than a K_b value of 3.6×10^6 M^{-1} reported for the dimeric complex of $[Ru_2(phen)_4(bmbh)]^{4+}$ {bmbh = 1,7-bis(4′-methyl-2,2′-bipyridin-4-yl)heptane} [17], approach 8.9×10^7 M^{-1} reported for the threading bis-intercalator of $[Ru_2(cpdppz)(phen)_4]^{4+}$ {cpdppz = *N*,*N*′-bis{12-cyano-12,13-dihydro-11*H*-cyclopenta[i]dipyrido[3,2-a:2′,3′-c]-phenazine-12-carboxmide-1,4-diaminobutane} [35]. The above mentioned facts indicate that **1**–**3** might bind to the DNA in a threading bis-intercalating mode.

3.2. Luminescence spectra

1–**3** in Tris–HCl buffer at room temperature were luminescent with maxima at 607, 608, and 612 nm, respectively, which were red-shifted relative to that reported for analogous mononuclear complex $[Ru(bpy)_2(p\text{-}mopip)]^{2+}$ (590 nm) [15]. Changes in emission spectra of **1**–**3** with increasing DNA concentrations are shown in Figs. 2, S3, and S4, respectively. As ct-DNA was added into the complex solutions, the emission intensities of **1** were almost undisturbed, while those of both **2** and **3** were increased by a factor of only <0.2. While Ji et al. reported that addition of the DNA resulted in sharp enhancements in the emission intensities by 0.9, 1.3, and 3.5 folds for $[Ru(bpy)_2(p\text{-}mopip)]^{2+}$, $[Ru(bpy)_2(p\text{-}hpip)]^{2+}$ and $[Ru(bpy)_2(p\text{-}npip)]^{2+}$ {p-npip = 2-(4-nitrophenyl)imidazo[4,5-*f*][1,10]phenanthroline} [15], respectively, which agrees with the order of their DNA binding constant values. Kelly [17] observed emission enhancement factors (I_{DNA}/I_{free}) of 2.08, 2.36, and 1.68 for dinuclear Ru(II) complexes of $[(phen)_2Ru(Mebpy)\text{-}(CH_2)_n\text{-}(bpyMe)Ru(phen)_2]^{4+}$ with n = 5, 7, and 10 in the presence of double-stranded DNA, respectively, which are less than or comparable to a factor of 2.4 for mononuclear analog of $[Ru(phen)_2(Me_2bpy)]^{2+}$ (Me_2bpy = 4, 4′-dimethyl-2,2′-bipyridyl).

$[Fe(CN)_6]^{4-}$ was used as the quencher in steady-state emission quenching experiments. As shown in Figs. 3, S5, and S6, the emissions of **1**–**3** were efficiently quenched by $[Fe(CN)_6]^{4-}$ in the absence of the DNA, resulting in almost linear Stern–Volmer plots with slopes of 1213 ± 9, 736 ± 10, and 550 ± 10 mM^{-1} for **1**, **2** and **3**, respectively. In the presence of the DNA, the slopes of the Stern–Volmer plots for **1**–**3** were drastically decreased to 110 ± 10, 56.9 ± 0.4, and 11.20 ± 0.2 mM^{-1}, corresponding to *R* values (the ratio of the slop in the absence of the DNA to that in the presence of DNA) of 11.0, 12.9, and 49.1, respectively. The *R* value has frequently been used to evaluate accessibility of the complexes to $[Fe(CN)_6]^{4-}$. The greater *R* value corresponds to more protection from emission quenching of the Ru(II) complex by DNA, due to the repulsion of the highly anionic $[Fe(CN)_6]^{4-}$ by the DNA polyanion [60–63]. Although the *R* values observed for **1**–**3** are qualitatively consistent with their DNA binding affinities, these values are only at the same order of magnitude as a *R* value of 20 reported for proven DNA intercalator, mononuclear analogous complex $[Ru(bpy)_2(pip)]^{2+}$ [42]. Obviously, **1**–**3** were efficiently protected from the quenching by $[Fe(CN)_6]^{4-}$ as they bond to the DNA, but less than anticipated from their DNA affinities, probably due to both the threading binding effect and hydrogen bonding formed between the oxygen atoms in the flexible linkers on **1**–**3** and the groove of the DNA [18] contributed to the DNA binding affinities but little on the shielding of **1**–**3**.

The competitive binding experiments with a well-established quenching experiment based on the displacement of the intercalating drug ethidium bromide (EB) from ct-DNA may give further information about the DNA binding properties of **1**–**3**. If a complex can displace EB from DNA-bound EB, the fluorescence of EB will be sharply decreased due to the fact that the free EB molecules are much less fluorescent than the DNA bound EB molecules because the surrounding water molecules quench the fluorescence of free EB, and **1**–**3** as

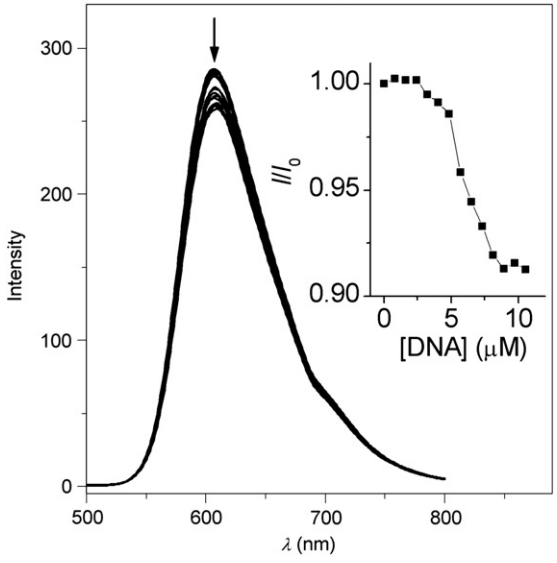

Fig. 2. Changes in emission spectra (λ_{ex} = 460 nm) of **1** (3 μM) with increasing concentrations of ct-DNA in 5 mM Tris–HCl buffer (pH = 7.10, 50 mM NaCl).

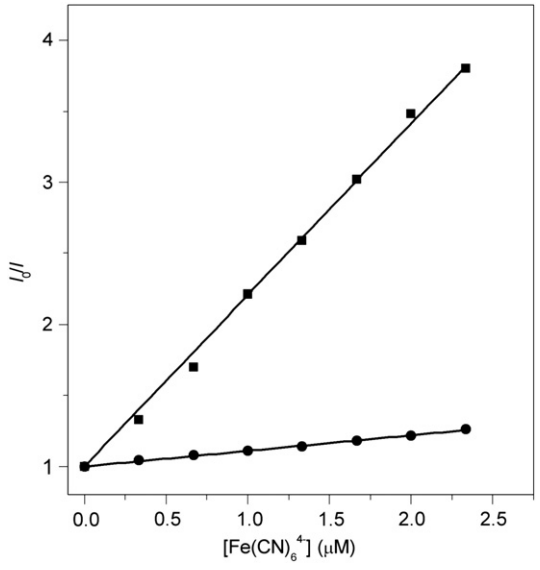

Fig. 3. Emission quenching of **1** with increasing concentrations of $[Fe(CN)_6]^{4-}$ in the absence (square) and presence (circle) of the DNA. [1] = 3 μM, [DNA]/[1] = 15.0.

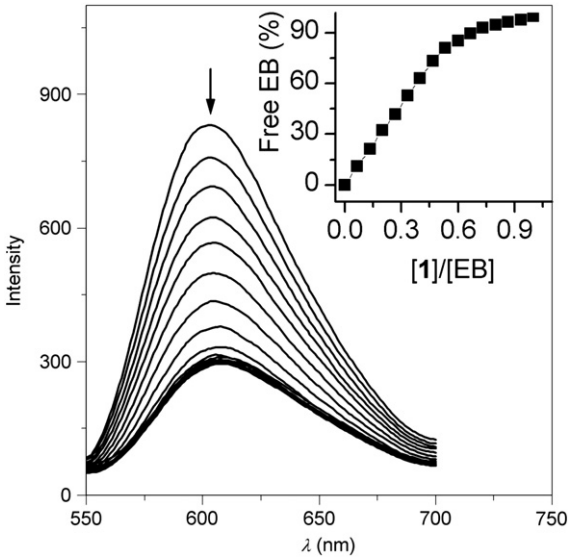

Fig. 4. Changes in emission spectra of EB bound to DNA upon successive additions of **1** (0–27 μM). The arrows show the intensity changes upon increasing concentrations of **1**. Inset: a plot of percentage of free EB vs [1]/[EB]. [EB] = 20 μM, [DNA] = 100 μM, λ_{ex} = 537 nm.

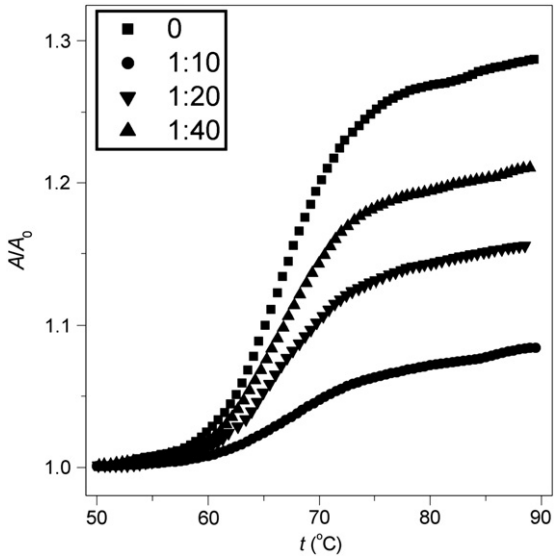

Fig. 5. Thermal denaturation curves of ct-DNA (100 μM) at varied concentration ratios of [**1**]/[DNA].

well as DNA bound **1**–**3** are also negligibly weakly emissive as excited at the excitation wavelength of EB (λ_{ex} = 537 nm) [64]. However, not only the DNA intercalators but also groove DNA binders could cause the reduction in the emission intensities of DNA bound EB [65], but only moderately for the latter case. As shown in Figs. 4, S7, and S8, a remarkable reduction in emission intensities by 68%, 71%, and 53% for **1**–**3** were achieved as **1**–**3** were added to EB–DNA system, characteristic for the intercalative binding of **1**–**3** to the DNA [66–68]. To further illustrate the DNA binding affinities of **1**–**3**, the values of the apparent DNA binding constant K_{app} were derived according to Eq. (3),

$$K_{app} = K_{EB}[EB]_{50\%} / [Ru]_{50\%} \quad (3)$$

where K_{EB} is the DNA binding constant of EB, and $[EB]_{50\%}$ and $[Ru]_{50\%}$ are the EB and Ru(II) complex concentrations at which 50% of EB were replaced from EB–DNA complex. In the plots of percentage of free EB vs [Ru]/[EB], we can see that 50% of the EB molecules were replaced from DNA-bound EB at concentration ratios of [Ru]/[EB] = 0.31, 0.21, and 0.18 for **1**, **2**, and **3** respectively, as shown in the insets of Figs. 4, S7, and S8. By taking a DNA binding constant value of 1.0×10^7 M^{-1} for EB [11,69], the values of the apparent DNA binding constant for **1**, **2**, and **3** were derived to be 3.2×10^7, 4.8×10^7 and 5.6×10^7 M^{-1}, respectively, which are in agreement with those derived by UV–vis absorption spectroscopy.

3.3. Thermal denaturation of ct-DNA

The DNA melting study is a further evidence for the intercalation of the Ru(II) complexes into the DNA helix. The DNA melting experiments were carried out to distinguish the different binding modes (binding by intercalation or binding externally). The intercalation of small molecules into the DNA double helix has been known to increase the helix melting temperature at which the double helix denatures into single stranded DNA. The melting of the helix can lead to an increase in the absorption at 260 nm, because the extinction coefficient of DNA bases at 260 nm in the double-helical form is much less than in the single strand form [64,70–74]. Thus, the helix-to-coil transition temperature can be determined by monitoring the absorbance of the DNA bases at 260 nm as a function of temperature. Although the increase in denaturation temperature is not specific of any particular type of noncovalent interaction, the ΔT_m values may give hints on the DNA binding mode. The DNA melting curves in the absence and presence of different concentrations of the Ru(II) complexes are presented in Figs. 5, S9, and S10. The T_m value of ct-DNA was found to be 67.1 °C in the absence of **1**–**3**, and was enhanced successively with increasing concentrations of **1**–**3**. The ΔT_m values at a concentration ratio of [DNA]/[Ru] = 10:1 were found to be 1.5, >15, and >15 °C for **1**–**3**, respectively. In comparison with the ΔT_m values reported for some DNA intercalative complexes shown in Table 2, the ΔT_m value for **2** and **3** are typical for DNA intercalators, and are reasonable as compared to a ΔT_m value of 20 ± 2 °C reported for the duplex 5′-TCGGGATCCCGA-3′ in the presence of a threading bis-intercalator of $[Ru_2(phen\text{-}5\text{-}SOS\text{-}5\text{-}phen)(dpq)_4]^{4+}$ at a relatively large Ru(II) complex concentration {[5′-TCGGGATCCCGA-3′]/[Ru] = 0.5}[18]. Although the other spectral evidences except for the thermal denaturation data seem in support of a threading intercalative DNA binding mode for **1**, the small ΔT_m value observed for **1** may be because the linker length of **1** is too short to facilitate the intercalation of the two Hpip moieties on L^1 of **1** between the base pairs of the DNA deeply. This lead us to draw a conclusion that "the threading effect" would make a dominant contribution to the DNA binding affinities observed for **1–3** compared to "the intercalative effect", while "the intercalative effect" directly affect the DNA denaturation temperature. It should also be emphasized that

Table 2
The comparisons of the values of DNA binding constant K_b and denaturation temperature difference ΔT_m.

DNA binder[a]	K_b (M^{-1})	[DNA]/[Ru]	ΔT_m (°C)	Ref.
EB	1.0×10^7	10	13	[65]
$[Ru(phen)_2(qdppz)]^{2+}$	$>1.0\times10^6$	25	6.0	[71]
$[Ru_2(phen\text{-}5\text{-}SOS\text{-}5\text{-}phen)(dpq)_4]^{4+}$	8.9×10^7	0.5	20[b]	[18]
$[Ru(phen)_2(hqdppz)]^{2+}$	1.0×10^5	25	6.0	[70]
$[Ru(NH_3)_4(pip)]^{2+}$	4.3×10^5	1.0	8.0	[72]
$[Ru(NH_3)_4(pip)]^{2+}$	9.7×10^5	1.0	8.0	[72]
$[Ru(bpy)(ppd)]^{2+}$	1.3×10^6	10	5.9	[73]
$[Ru(phen)_2(dppz)]^{2+}$	5.1×10^6	10	9.1	[74]
$[Ru(NH_3)_4(dppz)]^{2+}$	1.8×10^5	10	5.2	[74]
1	$(5.7\pm1.6)\times10^7$	10	1.5	This work
2	$(7.5\pm3.1)\times10^7$	10	>15	This work
3	$(9.5\pm2.5)\times10^7$	10	>15	This work

[a] See Abbreviations section. [b] [5′-TCGGGATCCCGA-3′]/[Ru] = 0.5

the magnitude of ΔT_m value does not invariably parallel the DNA binding affinities even for structurally similar drugs with considerably different DNA binding affinity, e.g. $[Ru(phen)_2(qdppz)]^{2+}$ {qdppz = naphtho[2,3-a]dipyrido[3,2-h:2′,3′-*f*]phenazine-5,18-dione} and $[Ru(phen)_2(hqdppz)]^{2+}$ {hqdppz = 5,18-dihydroxynaphtho[2,3-a]dipyrido[3,2-h:2′,3′-*f*]phenazine} were reported to exhibit almost same ΔT_m value of 6 °C at [DNA]/[Ru] = 25:1 [70], but their DNA binding constant values differed by one order of magnitude (see Table 2).

3.4. Viscosity measurements

Optical photophysical probes provide necessary, but not sufficient, clues to support a binding mode. Hydrodynamic measurements, such as viscosity measurements which are sensitive to length change, are regarded as the least ambiguous and the most critical tests of a binding mode in solution in the absence of crystallographic structural data [75,76]. To further explore the interaction properties between **1**–**3** and the DNA, the specific relative viscosities of the DNA were measured by adding increasing concentrations of **1**–**3** and known DNA intercalator ethidium bromide (EB) for comparison purpose. A classical intercalation mode results in lengthening the DNA helix, leading to an increase in the DNA viscosity. However, a partial or nonclassical intercalation of the ligand could bend (or kink) the DNA helix, reducing the effective length of the DNA, and therefore the DNA viscosities. In contrast, an electrostatic or grooving binding mode has little effects on the DNA viscosities [74,76]. As shown in Fig. 6, the viscosities of the ct-DNA increased upon successive additions of **1**–**3**, similarly to proven DNA intercalators of EB and previously reported mononuclear complex $[Ru(bpy)_2(p\text{-mopip})]^{2+}$ [15]. According to the values of DNA binding constant, **1**–**3** should result in more evident increases in DNA viscosities than $[Ru(bpy)_2(p\text{-mopip})]^{2+}$ and EB, since **1**–**3** has been evidenced to bind to the DNA more tightly than $[Ru(bpy)_2(p\text{-mopip})]^{2+}$ and EB. On the contrary, **1**–**3** were observed to induce smaller increases in the DNA viscosities than EB. We attribute these small viscosity increases in the presence of **1**–**3** with respect to EB, to that the threading effect of **1**–**3** fasten both ends of **1**–**3** onto the same strand of the DNA, preventing evidently lengthening the DNA helix and sharply increasing the DNA viscosities accordingly.

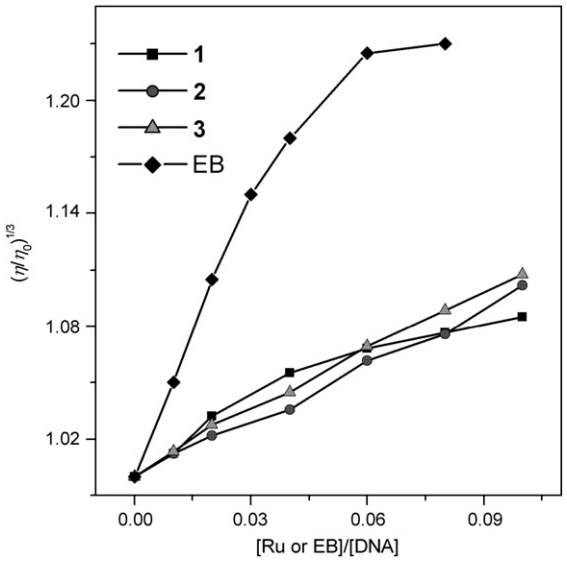

Fig. 6. Effects of increasing concentrations of **1**–**3** and EB on the relative viscosities of ct-DNA in buffered 50 mM NaCl at 32.04 ± 0.02 °C, [DNA] = 0.4 mM.

3.5. The optimized structures by density functional theory calculations

The optimized structures for **1**–**3** are shown in Fig. 7, and the computational selected bond lengths, bond angles, and dihedral angles of **1**–**3** using the DFT at the B3LYP/LanL2DZ level are shown in Table S1. The mean coordination bond lengths between the Ru and N atoms of the main ligand L^{1-3} ($Ru–N_m$), and between Ru and N atoms of the co-ligand bpy ($Ru–N_{co}$), and the mean coordination bond angles between the central Ru and two N atoms of the main ligand (A_m), and between the central Ru and two N atoms of the co-ligand (A_{co}) in **1**–**3** are found to be $Ru–N_m$ = 0.2119–0.2124 nm, $Ru–N_{co}$ = 0.2108–0.2116 nm, A_m = 78.38°–78.61° and A_{co} = 77.69°–77.92°, which are close to the corresponding data ($Ru–N_m$ = 0.2108 nm, $Ru–N_{co}$ = 0.2097 nm, A_m = 79.26° and A_{co} = 78.47°) previously reported for $[Ru(bpy)_2(pip)]$ [51], indicating that our computed results are reliable. Although **1**–**3** show some difference in linker orientations, the two Ru(II) centers for each of **1**–**3** seem to have ample separation for the orientation of the two pip moieties on **1**–**3** to thread the linkers and intercalate two pip moieties between the base pairs of the DNA.

4. Conclusion

UV–vis absorption spectroscopy and EB competitive binding experiments revealed that different lengths of flexible bridge-containing **1**–**3** avidly bound to ct-DNA with DNA binding constant values on the order of magnitude of $10^7\ M^{-1}$, three orders of magnitude greater than that reported for analogous mononuclear complex of $[Ru(bpy)_2(p\text{-mopip})]^{2+}$. Emission spectrophotometric DNA titrations, steady state emission quenching and DNA viscosity measurements demonstrated that the intercalation depth or the extent of protection of **1**–**3** by the DNA are similar to those of $[Ru(bpy)_2(p\text{-mopip})]^{2+}$. The much enhanced DNA binding affinities and comparable intercalation depth compared to their mononuclear analogous complex $[Ru(bpy)_2(p\text{-mopip})]^{2+}$ led us to make a conclusion that **1**–**3** bound to the DNA probably in a threading intercalation binding mode, and the threading effect made a dominant contribution to the DNA binding affinities, but little to the their protection from emission quenching and the lengthening of the DNA double strands.

Abbreviations

bpy	2,2′-bipyridine
bmbh	1,7-bis(4′-methyl-2,2′-bipyridin-4-yl)heptane
cpdppz	*N,N*′-bis{12-cyano-12,13-dihydro-11H-cyclopenta[i] dipyrido[3,2-a:2′,3′-c]phenazine-12-carboxamide}-1,4-diaminobutane
DFT	density functional theory
ct-DNA	calf thymus DNA
dppz	dipyrido[3,2-a:2′,3′-c]phenazine
dpq	pyrazino[2,3-*f*][1,10]phenanthroline
ebipcH	N-ethyl-4,7-bis([1,10]-phenanthroline[5,6-*f*]imidazol-2-yl) carbazole
EB	ethidium bromide
p-hpip	2-(p-hydroxyphenyl)imidazo[4,5-*f*][1,10]phenanthroline
hqdpp	5,18-dihydroxynaphtho[2,3-a]dipyrido[3,2-h:2′,3′-*f*] phenazine
L^1	1,2-bis(4-(1H-imidazo[4,5-*f*][1,10]phenanthrolin-2-yl) phenoxy)ethane
L^2	4,4′-[oxybis(2,1-ethanediyloxy)]bis-1H-Imidazo[4,5-*f*] [1,10]phenanthroline
L^3	2,2′-[1,2-ethanediylbis(oxy-2,1-ethanediyloxy-4,1-phenylene)]bis-1H- imidazo[4,5-*f*][1,10]phenanthroline
mebpy	4-methyl-2,2′-bipyridyl-4′-
MLCT	metal-to-ligand charge transfer
p-mopip	2-(4-methoxylphenyl)imidazo[4,5-*f*][1,10]phenanthroline
p-npip	2-(4-nitrophenyl)imidazo[4,5-*f*][1,10]phenanthroline

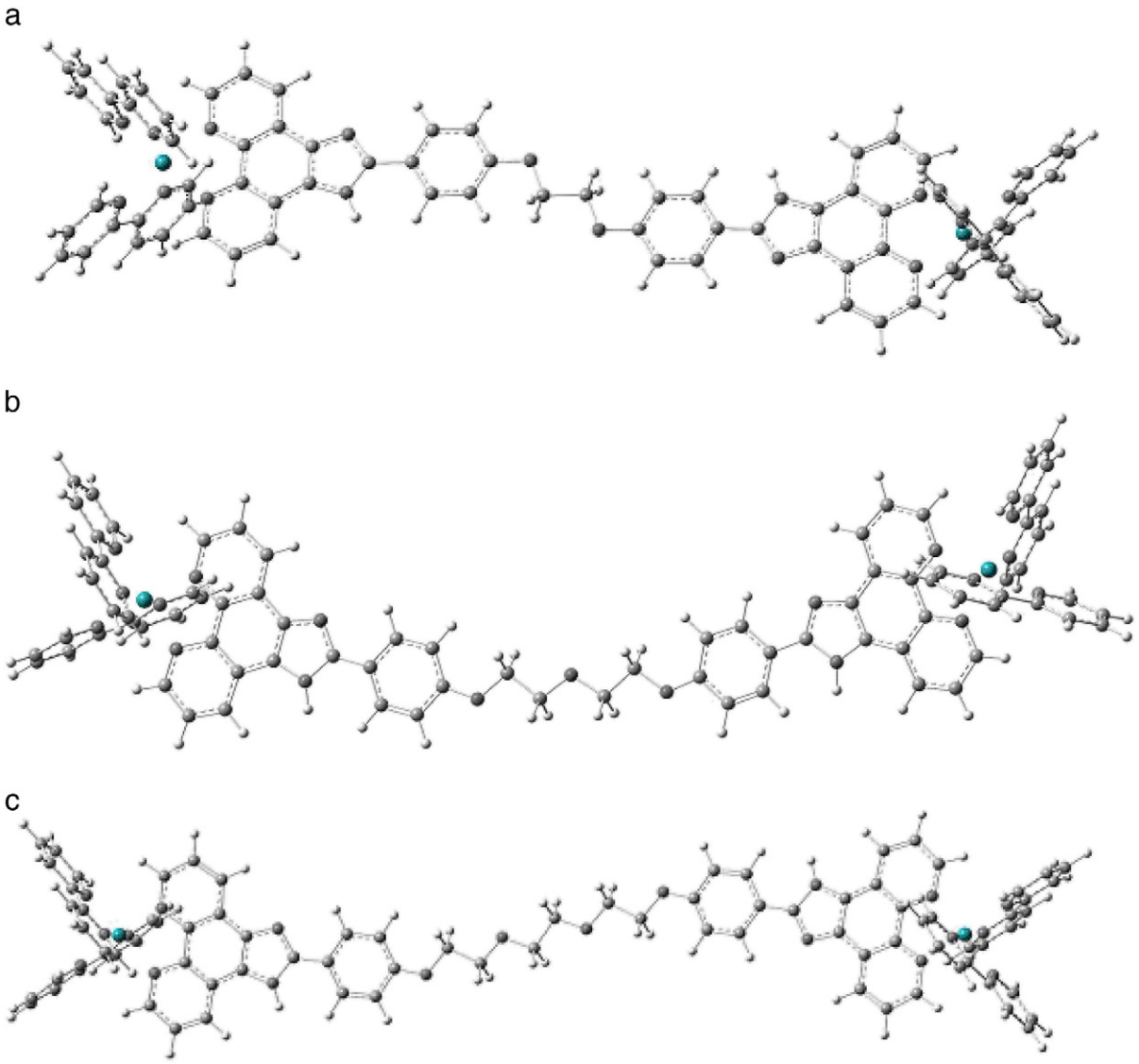

Fig. 7. Optimized structures of **1** (a), **2** (b) and **3** (c).

phen	1,10-phenanthroline
pip	2-phenylimidazo[4,5-*f*][1,10] phenanthroline
ppd	pteridino[7,6-*f*][1,10]phenanthroline-1,13(10H,12H)-dione
qdppz	naphtho[2,3-a]dipyrido[3,2-h:2′,3′-*f*]phenazine-5,18-dione
SOS	2-mercaptoethyl ether
TsCl	p-toluenesulfonyl chloride
UV-vis	UV-visible
1	$[Ru_2(bpy)_4(L^1)](ClO_4)_4$
2	$[Ru_2(bpy)_4(L^2)](ClO_4)_4$
3	$[Ru_2(bpy)_4(L^3)](ClO_4)_4$

Acknowledgements

The authors thank Professor Kang-Cheng Zheng for helpful guidance for the theoretical calculations, and the National Natural Science Foundation (Nos. 20971016, 20771016, 90922004), Beijing Natural Science Foundation (2072011), the Fundamental Research Funds for the Central Universities, and Measurements Fund of Beijing Normal University for financial supports.

Appendix A. Supplementary materials

Supplementary data to this article can be found online at doi:10.1016/j.jinorgbio.2010.12.004.

References

[1] C. Metcalfe, J.A. Thomas, Chem. Soc. Rev. 32 (2003) 215–224.
[2] E. Ruba, J.R. Hart, J.K. Barton, Inorg. Chem. 43 (2004) 4570–4578.
[3] K.E. Duncan, D.T. Odom, J.K. Barton, Chem. Rev. 99 (1999) 2797–2816.
[4] L.N. Ji, X.H. Zhou, J.G. Liu, Coord. Chem. Rev. 216 (2001) 513–536.
[5] Y. Liu, A. Chouai, N.N. Degtyareva, D.A. Lutterman, K.R. Dunbar, C. Turro, J. Am. Chem. Soc. 127 (2005) 10796–10797.
[6] J. Olofsson, L.M. Wilhelmsson, P. Lincoln, J. Am. Chem. Soc. 126 (2004) 15458–15465.
[7] I. Haq, P. Lincoln, D. Suh, B. Norden, B.Z. Chowdhry, J.B. Chaires, J. Am. Chem. Soc. 117 (1995) 4788–4796.
[8] C. Moucheron, A. Kirsch-De Mesmaeker, S. Choua, Inorg. Chem. 36 (1997) 584–592.
[9] J.G. Collins, J.R. Aldrich-Wright, I.D. Greguric, P.A. Pellegrini, Inorg. Chem. 38 (1999) 5502–5509.
[10] Y.M. Chen, Y.J. Liu, Q. Li, K.Z. Wang, J. Inorg. Biochem. 103 (2009) 1395–1404.
[11] M.J. Han, L.H. Gao, Y.Y. Lü, K.Z. Wang, J. Phys. Chem. B 110 (2006) 2364–2371.
[12] M.J. Han, Z.M. Duan, Q. Hao, S.Z. Zheng, K.Z. Wang, J. Phys. Chem. C 111 (2007) 16577–16585.
[13] G.Y. Bai, K.Z. Wang, Z.M. Duan, L.H. Gao, J. Inorg. Biochem. 98 (2004) 1017–1022.
[14] M.J. Han, L.H. Gao, K.Z. Wang, New J. Chem. 30 (2006) 208–214.

[15] J. Liu, W.J. Mei, L.J. Lin, K.C. Zheng, H. Chao, F.C. Yun, L.N. Ji, Inorg. Chim. Acta 357 (2004) 285–293.
[16] H.J. Han, Y.M. Chen, K.Z. Wang, New J. Chem. 32 (2008) 970–980.
[17] F.M. O'Reilly, J.M. Kelly, New J. Chem. 22 (1998) 215–217.
[18] J. Aldrich-Wright, C. Brodie, E.C. Glazer, N.W. Luedtke, L. Elson-Schwab, Y. Tor, Chem. Commun. (2004) 1018–1019.
[19] R.H. Terbrueggen, J.K. Barton, Biochemistry 34 (1995) 8227–8234.
[20] S. Delaney, M. Pascaly, P.K. Bhattacharya, K. Han, J.K. Barton, Inorg. Chem. 41 (2002) 1966–1974.
[21] C. Rajput, R. Rutkaite, L. Swanson, I. Haq, J.A. Thomas, Chem. Eur. J. 12 (2006) 4611–4619.
[22] H. Chao, Y.X. Yuan, F. Zhou, L.N. Ji, Transit. Met. Chem. 31 (2006) 465–469.
[23] C.R.K. Glasson, G.V. Meehan, J.K. Clegg, L.F. Lindoy, J.A. Smith, F.R. Keene, C. Motti, Chem. Eur. J. 14 (2008) 10535–10538.
[24] H. Chao, R.H. Li, C.W. Jiang, H. Li, L.N. Ji, X.Y. Li, J. Chem. Soc., Dalton Trans. (2001) 1920–1926.
[25] H. Chao, B.H. Ye, H. Li, R.H. Li, J.Y. Zhao, L.N. Ji, Polyhedron 19 (2000) 1975–1983.
[26] S. Rani-Beeram, K. Meyer, A. McCrate, Y. Hong, M. Nielsen, S. Swavey, Inorg. Chem. 47 (2008) 11278–11283.
[27] F. Westerlund, M.P. Eng, M.U. Winters, P. Lincoln, J. Phys. Chem. B 111 (2007) 310–317.
[28] F.R. Liu, K.Z. Wang, G.Y. Bai, Y.A. Zhang, L.H. Gao, Inorg. Chem. 43 (2004) 1799–1806.
[29] C.W. Jiang, H. Chao, X.L. Hong, H. Li, W.J. Mei, L.N. Ji, Inorg. Chem. Commun. 6 (2003) 773–775.
[30] U. McDonnell, M.R. Hicks, M.J. Hannon, A. Rodger, J. Inorg. Biochem. 102 (2008) 2052–2059.
[31] T.K. Janaratne, A. Yadav, F. Ongeri, F.M. MacDonnell, Inorg. Chem. 46 (2007) 3420–3422.
[32] B.T. Patterson, J.G. Collins, F.M. Foley, F.R. Keene, J. Chem. Soc., Dalton Trans. (2002) 4343–4350.
[33] J.A. Smith, J.G. Collins, B.T. Patterson, F.R. Keene, Dalton Trans. (2004) 1277–1283.
[34] J.Z. Wu, L. Yuan, J. Inorg. Biochem. 98 (2004) 41–45.
[35] B. Önfelt, P. Lincoln, B. Nordén, J. Am. Chem. Soc. 123 (2001) 3630–3637.
[36] J.L. Morgan, C.B. Spillane, J.A. Smith, D.P. Buck, J.G. Collins, F.R. Keene, Dalton Trans. (2007) 4333–4342.
[37] Y. Nakabayashi, N. Iwamoto, H. Inada, O. Yamauchi, Inorg. Chem. Commun. 9 (2006) 1033–1036.
[38] S.P. Foxon, T. Phillips, M.R. Gill, M. Towrie, A.W. Parker, M. Webb, J.A. Thomas, Angew. Chem. Int. Ed. 46 (2007) 3686–3688.
[39] G.I. Pascu, A.C.G. Hotze, C. Sanchez-Cano, B.M. Kariuki, M.J. Hannon, Angew. Chem. Int. Ed. 46 (2007) 4374–4378.
[40] J. Malina, M.J. Hannon, V. Brabec, Chem. Eur. J. 14 (2008) 10408–10414.
[41] V. Gonzalez, T. Wilson, I. Kurihara, A. Imai, J.A. Thomas, J. Otsuki, Chem. Commun. (2008) 1868–1870.
[42] L.N. Ji, J.G. Liu, B.H. Ye, Mater. Sci. Eng., C 10 (1999) 51–57.
[43] J. Bolger, A. Goarden, E. Ishow, J.P. Launay, Inorg. Chem. 35 (1996) 2937–2944.
[44] J.V. Houten, R.J. Watts, J. Am. Chem. Soc. 98 (1976) 4853–4858.
[45] Y. Liu, Z.Y. Duan, H.Y. Zhang, X.L. Jiang, J.R. Han, J. Org. Chem. 70 (2005) 1450–1455.
[46] M.F. Reichmann, S.A. Rice, C.A. Thomas, P. Doty, J. Am. Chem. Soc. 76 (1954) 3047–3053.
[47] J. Marmur, J. Mol. Biol. 3 (1961) 208–211.
[48] S.R. Smith, G.A. Neyhart, W.A. Kalsbeck, H.H. Thorp, New J. Chem. 18 (1994) 397–406.
[49] M.T. Carter, M. Rodriguez, A.J. Bard, J. Am. Chem. Soc. 111 (1989) 8901–8911.
[50] J.B. Chaires, N. Dattagupta, D.M. Crothers, Biochemistry 21 (1982) 3933–3940.
[51] K.C. Zheng, H. Deng, X.W. Liu, H. Li, H. Chao, L.N. Ji, J. Mol. Struct. 682 (2004) 225–233, (Theochem).
[52] A. Gorling, Phys. Rev. 54 (1996) 3912–3915.
[53] P.J. Hay, W.R. Wadt, J. Chem. Phys. 82 (1985) 270–283.
[54] A. Juris, V. Balzani, F. Barigelletti, S. Campagna, P. Belser, A.V. Zelewsky, Coord. Chem. Rev. 84 (1988) 85–227.
[55] M.J. Frisch, G.W. Trucks, H.B. Schlegel, G.E. Scuseria, M.A. Robb, J.R. Cheeseman, J.A. Montgomery, Jr., T. Vreven, K.N. Kudin, J.C. Burant, J.M. Millam, S.S. Iyengar, J. Tomasi, V. Barone, B. Mennucci, M. Cossi, G. Scalmani, N. Rega, G.A. Petersson, H. Nakatsuji, M. Hada, M. Ehara, K. Toyota, R. Fukuda, J. Hasegawa, M. Ishida, T. Nakajima, Y. Honda, O. Kitao, H. Nakai, M. Klene, X. Li, J.E. Knox, H.P. Hratchian, J.B. Cross, C. Adamo, J. Jaramillo, R. Gomperts, R.E. Stratmann, O. Yazyev, A.J. Austin, R. Cammi, C. Pomelli, J.W. Ochterski, P.Y. Ayala, K. Morokuma, G.A. Voth, P. Salvador, J. J. Dannenberg, V.G. Zakrzewski, S. Dapprich, A.D. Daniels, M.C. Strain, O. Farkas, D. K. Malick, A.D. Rabuck, K. Raghavachari, J.B. Foresman, J.V. Ortiz, Q. Cui, A.G. Baboul, S. Clifford, J. Cioslowski, B.B. Stefanov, G. Liu, A. Liashenko, P. Piskorz, I. Komaromi, R.L. Martin, D.J. Fox, T. Keith, M.A. Al-Laham, C.Y. Peng, A. Nanayakkara, M. Challacombe, P.M. W. Gill, B. Johnson, W. Chen, M. W. Wong, C. Gonzalez, and J.A. Pople, Gaussian, Inc., Pittsburgh PA, 2003.
[56] Z. Ji, S. Huang, A.R. Guadalupe, Inorg. Chim. Acta 305 (2000) 127–134.
[57] X.H. Zhou, B.H. Ye, H. Li, J.G. Liu, Y. Xiang, L.N. Ji, J. Chem. Soc. Dalton Trans. (1999) 1423–1428.
[58] C. Hiort, P. Lincoln, B. Nordén, J. Am. Chem. Soc. 115 (1993) 3448–3454.
[59] A.M. Pyle, J.P. Rehmann, R. Meshoyrer, C.V. Kumar, N.J. Turro, J.K. Barton, J. Am. Chem. Soc. 111 (1989) 3051–3058.
[60] C.V. Kumar, J.K. Barton, N.J. Turro, J. Am. Chem. Soc. 107 (1985) 5518–5523.
[61] W.J. Mei, J. Liu, K.C. Zheng, L.J. Lin, H. Chao, A.X. Li, F.C. Yun, L.N. Ji, Dalton Trans. (2003) 1352–1359.
[62] J.G. Liu, Q.L. Zhang, X.F. Shi, L.N. Ji, Inorg. Chem. 40 (2001) 5045–5050.
[63] I. Haq, P. Lincoln, D. Suh, B. Norden, B.Z. Chowdrey, J.B. Chaires, J. Am. Chem. Soc. 117 (1995) 4788–4796.
[64] I. Ortmans, B. Elias, J.M. Kelly, C. Moucheron, A.K. Demesmaeker, Dalton Trans. (2004) 668–676.
[65] J.M. Kelly, A.B. Tossi, D.J. Meconnell, C. Ohuigin, Nucleic Acids Res. 13 (1985) 6017–6034.
[66] Y.Z. Ma, H.J. Yin, K.Z. Wang, J. Phys. Chem. B 113 (2009) 11039–11047.
[67] Y.Y. Lü, L.H. Gao, M.J. Han, K.Z. Wang, Eur. J. Inorg. Chem. (2006) 430–436.
[68] B.Y. Wu, L.H. Gao, Z.M. Duan, K.Z. Wang, J. Inorg. Biochem. 99 (2005) 1685–1691.
[69] D.L. Boger, B.E. Fink, S.R. Brunette, W.C. Tse, M.P. Hedrick, J. Am. Chem. Soc. 123 (2001) 5878–5891.
[70] M. Cory, D.D. Mckee, J. Kagan, D.W. Henry, J.A. Miller, J. Am. Chem. Soc. 107 (1985) 2528–2536.
[71] A. Ambroise, B.G. Maiya, Inorg. Chem. 39 (2000) 4256–4263.
[72] P.U. Maheswari, M. Palaniandavar, J. Inorg. Biochem. 98 (2004) 219–230.
[73] F. Gao, H. Chao, F. Zhou, Y.X. Yuan, B. Peng, L.N. Ji, J. Inorg. Biochem. 100 (2006) 1487–1494.
[74] R.B. Nair, E.S. Teng, S.L. Kirkland, C.J. Murphy, Inorg. Chem. 37 (1998) 139–141.
[75] S. Satyanarayana, J.C. Dabrowiak, J.B. Chaires, Biochemistry 31 (1992) 9319–9324.
[76] S. Satyanarayana, J.C. Dabrowiak, J.B. Chaires, Biochemistry 32 (1993) 2573–2584.